Role of Surfactant in Composite Latex Particle Morphology

Y. C. CHEN, VICTORIA DIMONIE, and MOHAMED S. EL-AASSER

Emulsion Polymers Institute, Center for Polymer Science and Engineering and Department of Chemical Engineering, Lehigh University, Bethlehem, Pennsylvania 18015

SYNOPSIS

Composite particles were prepared by seeded emulsion polymerization at 70°C using $K_2S_2O_8$ as initiator and two different nonionic surfactants. Monodisperse polystyrene latex particles were used as seed and methyl methacrylate was used as second-stage monomer. When the surfactant, polyethylene oxide–propylene oxide (Pluronic F-108), was used, the final particle morphology showed that the PMMA (core) was partially covered by polystyrene. However, when nonyphenol polyethylene oxide (Igepal Co-990) was used as surfactant, one observed a reversed type of encapsulation (i.e., PS core is partially engulfed by PMMA). The interfacial tensions of the polymer phase against water containing the appropriate surfactant were measured by the drop-volume method and used in a mathematical model based on thermodynamic analysis to predict the equilibrium particle morphology. The observed particle morphologies were found to differ from the predicted morphologies at low conversion of the second-stage monomer but agreed with it at higher conversion.

INTRODUCTION

Control of composite latex particle morphology is important for many latex applications such as adhesives, coatings, impact modification, and toughening of polymer matrices. Composite latex particles are usually prepared by seeded emulsion polymerization techniques where a second-stage monomer is polymerized in the presence of seed latex particles. During the course of seeded emulsion polymerization, thermodynamic factors determine the equilibrium morphology of the final composite latex particle, and the kinetic factors determine the ease with which such thermodynamically favored morphology can be achieved.[1]

In terms of thermodynamics, based on the minimum surface free energy change principle, polymer phase–water and polymer phase–polymer phase interfacial tensions have been proved as key parameters in deciding the thermodynamically preferred morphology.[1-3] Therefore, any factor affecting the interfacial tensions of polymer phases are thought to be able to change the composite latex particle morphology. Kinetic parameters such as the viscosity at the polymerization loci, polymer molecular weights, the mode of second-stage monomer addition, and their impact on particle morphology have also been observed.[1-5]

In the preparation of composite latexes, surfactants are usually required to increase the colloidal stability of the particles. The existence of surfactant molecules at the interface between the polymer phase and the aqueous phase may greatly affect the interfacial tension at the polymer phase–water interface, and therefore the particle morphology. In the present work, this phenomenon is investigated. For this purpose the particle morphology of two systems of composite particles polystyrene–poly(methyl methacrylate), which differed only in the type of surfactant used, were studied. In addition, the development of particle morphology during the course of seeded emulsion polymerization were investigated.

THERMODYNAMIC BACKGROUND

The thermodynamic analysis that will be considered for determining the latex particle morphology is based on the approach presented 20 years ago by Torza and Mason.[6] They studied the interfacial be-

Journal of Applied Polymer Science, Vol. 45, 487–499 (1992)
 CCC 0021-8995/92/030487-13$04.00

havior of systems containing three mutually immiscible liquids. In this case the thermodynamics of the system was critical since the liquid phase was highly mobile, i.e., low viscosity. They examined the conditions necessary for a coacervate droplet (liquid 3) to engulf an initial droplet (liquid 1) when both are immersed in a continuous phase (liquid 2) by the spreading coefficient, S, which is defined as

$$S_i = \gamma_{jk} - (\gamma_{ij} + \gamma_{ik}) \quad (1)$$

By assuming that the interfacial tension of liquid 1 against liquid 2 (γ_{12}) is greater than that of liquid 3 against liquid 2 (γ_{23}), only three possible sets of values for S exist. These correspond to the three different equilibrium configurations: complete engulfing (core–shell), partial engulfing (hemisphere), and nonengulfing (individual particle). Complete engulfing occurs only if $S_3 > 0$, $S_2 < 0$, and $S_1 < 0$. On the other hand, when $S_2 < 0$, $S_3 < 0$, and $S_1 < 0$ partial engulfing was preferred. Torza and Mason demonstrated the general validity of their approach by making a number of interfacial tension measurements, calculating values of S, and then observing what occurred in the actual three-phase system. In most cases prediction of engulfing based on S were satisfactory. This approach should be broadly applicable in determining when engulfing will occur

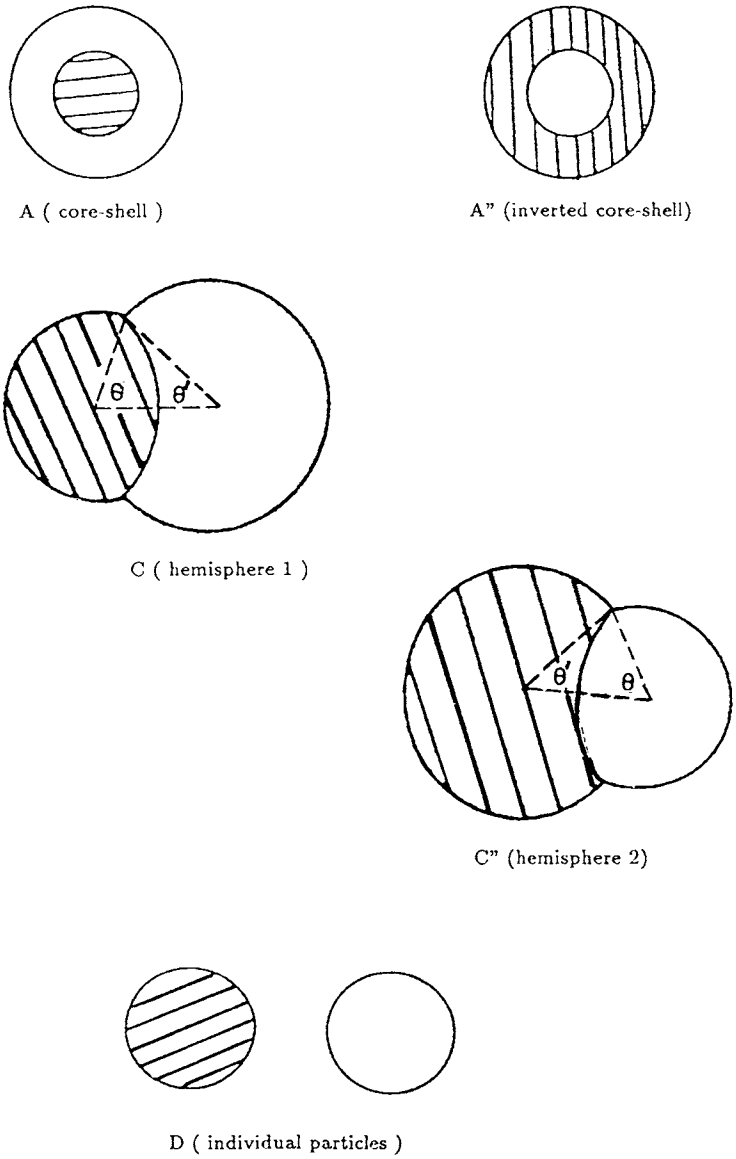

Figure 1 Various morphological structures of particles dispersed in water. (Hatched area, polymer 1; open area, polymer 2).

in various encapsulation systems. Recently, Sundberg et al.[7] by applying Torza and Mason's approach presented a thermodynamic analysis of the morphology of a relatively large size oil droplet in the micrometer range encapsulated by a polymer. Their analysis revealed that the interfacial tension of each phase is the key factor governing the type of microcapsules formed (core–shell, hemispheres, or individual particles).

In our previous work[1,2] a thermodynamic analysis similar to that presented by Sundberg et al.[7] and a mathematical model were derived to describe the free energy changes corresponding to various composite latex particle morphologies shown in Figure 1. The methodology involves consideration of the free energy changes for the following hypothetical pathways. The initial state was considered to consist of a polymer phase 1 (seed particles of polymer 1 swollen by the second-stage monomer, i.e., monomer 2) suspended in water containing surfactant. The final state is one of the morphologies shown in Figure 1. The only contribution to the free energy change for this pathway is the creation of new interfaces and changes in the corresponding interfacial tensions. For latex particles dispersed in a continuous water phase, those interfaces include polymer phase 1–water, polymer phase 2–water, and polymer phase 1–polymer phase 2. Polymer phase 2 is polymer 2 (formed as a result of the polymerization of monomer 2 in the presence of polymer 1) swollen by its own monomer. The total concentration of monomer 2 is dependent on the conversion. The monomer distribution between polymer 1 and polymer 2 is assumed to be proportional to the volume fraction of each polymer.[8,9] The total free energy change for all types of configurations shown in Figure 1 can be expressed as

$$\Delta G = \Sigma \gamma_{ij} A_{ij} - \gamma_0 A_0 \tag{2}$$

where γ_{ij} is the interfacial tension between i and j and A_{ij} the corresponding interfacial area, γ_0 is the interfacial tension of original polymer phase 1 (i.e., seed particles of polymer 1 swollen by monomer 2) suspended in water phase, and A_0 is its interfacial area. The results of free energy change equations for each case shown in Figure 1 are summarized in Table I. The thermodynamically preferred mor-

Table I Free Energy Changes for Various Morphological Structures of Latex Particles Dispersed in Water

CASE	$\Delta\psi$ (Surface Energy/Area)	Equation No.
A (core–shell)	$F[\gamma_{12}(V_r + 1)^{-2/3} + \gamma_{2w}] - \gamma_{1w}Y$	(3)
A″ (inverted core–shell)	$F[\gamma_{12}(V_r^{-1} + 1)^{-2/3} + \gamma_{1w}] - \gamma_{1w}Y$	(4)
C (hemisphere 1)	$(F/2)\{(V_r + 1)^{-2/3}\gamma_{1w}(1 + \cos\theta) + (V_r + 1)^{-2/3}(1 - \cos\theta)\gamma_{12} + (R_2/R)^2(1 + \cos\theta')\gamma_{2w}\} - \gamma_{1w}Y$	(5)
	$(R_2/R)^3 = \dfrac{1 - (V_r + 1)^{-1}\{1 - (\frac{1}{8})(1 - \cos\theta)[3\sin^2\theta + (1 - \cos\theta)^2]\}}{1 - (\frac{1}{8})(1 - \cos\theta')[3\sin^2\theta' + (1 - \cos\theta')^2]}$	(6)
	$R_2/R = (V_r + 1)^{-1/3}\sin\theta/\sin\theta'$	(7)
C″ (hemisphere 2)	$(F/2)\{(R_1/R)^2(1 + \cos\theta')\gamma_{1w} + \gamma_{12}(1 - \cos\theta)(V_r^{-1} + 1)^{-2/3} + (V_r^{-1} + 1)^{-2/3}(1 + \cos\theta)\gamma_{2w}\} - \gamma_{1w}Y$	(8)
	$(R_1/R)^3 = \dfrac{1 - (V_r^{-1} + 1)\{1 - (\frac{1}{8})(1 - \cos\theta)[3\sin^2\theta + (1 - \cos\theta)^2]\}}{1 - (\frac{1}{8})(1 - \cos\theta')[3\sin^2\theta' + (1 - \cos\theta')^2]}$	(9)
	$R_1/R = (V_r^{-1} + 1)^{-1/3}\sin\theta/\sin\theta'$	(10)
D (individual particles)	$F(\gamma_{1w} + \gamma_{2w}V_r^{2/3})(V_r + 1)^{-2/3} - \gamma_{1w}Y$	(11)

where $Y = K(V_f + 2)^{-2/3}$, $K = (1 + W_r d_1/d_{2m})^{2/3}$, $V_f = W_r d_1/d_2$ and $F = [Y^{3/2} + (1 - d_2/d_{2m})X/(1 + 1/V_f)]^{2/3}$. d_1, d_2, and d_{2m} are the densities of polymer 1, polymer 2, and monomer 2, respectively. W_r is weight ratio of total monomer 2 to polymer 1. X is polymerization conversion. R_1, R_2, and R are the radii of polymer phase 1, polymer phase 2, and the overall composite particle, respectively. θ or θ' (see Fig. 1) are the angles bewteen the line that connects the two centers of the hemispheres and the other line that connects the centers and the three-phase point. γ_{12}, γ_{1w}, and γ_{2w} are interfacial tensions between the two polymer phases; polymer phase 1 and water (containing surfactant, if present), and polymer phase 2 and water (containing surfactant, if present), respectively. A polymer phase is defined as polymer 1 or 2 dissolved in MMA monomer. V_r is the volume ratio of polymer phase 2 to polymer phase 1.

phology will be the one that has the minimum interfacial free energy change. Calculation of the free energy change by the equations listed in Table I involves a trial-and-error solution method. A FORTRAN77 computer program was prepared for this purpose. The calculation of the free energy changes requires knowledge of three interfacial tensions; polymer phases 1 and 2 against the aqueous phase, and polymer phase 1 against polymer phase 2. This thermodynamic analysis approach has been used to predict the particle morphology in composite latex particles and the influence of synthesis parameters, such as monomer–polymer ratio, and type of initiator.[1,2] However, it should be noted that the kinetic parameters prevailing during the course of polymerization will determine whether or not the thermodynamic equilibrium predicted morphology is attained. The kinetic parameters may influence the local viscosity, chain entanglements, grafting, or even crosslinking reactions. These effects will hinder or retard the rate of chain mobility, and as such will hinder or retard attainment of the equilibrium morphology.

It should be noted that the practical need of stabilizing agents and initiator[2,10] in emulsion polymerization may greatly affect the interfacial tension at the polymer phase–water interface and, therefore, particle morphology. The results of the influence of monomer–polymer ratio and initiator type have been reported in previous papers.[1,2] This study is devoted to the influence of surfactant type on particle morphology.

EXPERIMENTAL

Materials

The monodisperse polystyrene (PS) latex, LS 1102A (the Dow Chemical Co.) was used as seed. The PS latex was cleaned by the serum replacement technique until the conductivity of the serum emerging from the filtration cell was close to that of distilled deionized (DDI) water. The monomer methyl methacrylate (Rohm and Haas Co.) was washed with 10% aqueous sodium hydroxide solution, followed by water, dried overnight (at 5°C) with anhydrous sodium sulfate (100 g/L), and vacuum distilled under dry nitrogen to remove the inhibitor. All other materials were used as received including potassium persulfate initiator ($K_2S_2O_8$, Fisher Scientific Co.), Igepal Co-990 surfactant (nonylphenol polyethylene oxide, 100 mol ethylene oxide, GAF Co.), Pluronic F-108 (polyethylene oxide–propylene oxide, 80% polyoxyethylene, BASF/Wyandotte), and Areosol MA-80 emulsifier (sodium dihexyl sulfosuccinate, American Cyanamid Co.). Distilled deionized water was used in all polymerizations.

Seeded Emulsion Polymerization and Particle Morphology

Table II gives the standard recipe used in the preparation of the two composite latex systems with seed–monomer weight ratios of 30/70. One system, PS190/PMMA/Pluronic, used Pluronic F-108 as surfactant, the other one, PS/PMMA/Igepal, used Igepal Co-990 as surfactant.

Composite latexes were prepared by batch seeded emulsion polymerization using Dow LS1102A (denoted as PS190), monodisperse polystyrene latex as seed. The appropriate type and amount of surfactant was added to the "cleaned" seed latex and allowed to adsorb on the particle surface. Methyl methacrylate monomer was used in the second-stage polymerization. The seed particles were swelled by methyl methacrylate at room temperature for one hour, and then the second-stage polymerization was carried out at 70°C using potassium persulfate initiator in a magnetically stirred polymerization bottle.

The evolution of the particle morphology during the course of polymerization was examined by transmission electron microscopy (TEM) using two different methods. The first method involved examination of the "dry" latex particle morphology. A sample of composite latex particles was taken during the polymerization and placed on a grid, and almost instantaneously dried in a high vacuum chamber at room temperature. The morphology of the composite latex particles was examined by TEM after preferential staining of the polystyrene domains with RuO_4 vapor and negative staining with

Table II Recipe for Seeded Emulsion Polymerization of 30/70 Weight Ratio of Polystyrene Seed–Methyl Methacrylate Monomer

Ingredients	Weight (g)
PS seed particle	1.0
Surfactant	Variable[a]
Methyl methacrylate	2.35
DDI Water	11.0
$K_2S_2O_8$	0.0118

[a] For PS190/PMMA/Pluronic system: 0.366% based on water; for PS190/PMMA/Igepal system: 0.8% based on water.

Table III Recipe for Poly(methyl Methacrylate) Latex PMMA-KS

Ingredients	Weight (g)
Methyl methacrylate	40.35
Aerosol MA-80	1.4
DDI Water	156.64
$NaHCO_3$	0.252
$K_2S_2O_8$	0.204

phosphotungstic acid (PTA).[11] The second method involved examination of the particle morphology "embedded in ice"; a sample of the composite latex taken during the polymerization was frozen by liquid nitrogen and then examined by TEM.[12,13]

Preparation of Poly(methyl Methacrylate), PMMA-KS, Latex

PMMA-KS homopolymer latex was prepared by emulsion polymerization at 70°C, in the absence of seed particles, using the recipe given in Table III. In order to avoid any interference in the interfacial properties of PMMA-KS homopolymer due to eventual grafting of the nonionic surfactant, an anionic surfactant Aerosol MA-80 was used for the synthesis. The initiator–monomer ratio was the same as that used in the preparation of composite latexes. This homopolymer was used in the interfacial tension measurements representing the second-stage polymer in the composite latexes. The PMMA-KS latex particles were first cleaned by an ion exchange technique in order to remove the surfactant molecules and electrolytes and then dried out at room temperature before use.

Polymer Phase–Water Interfacial Tension Measurement

The interfacial tension measurements at room temperature were done by the drop-volume method[14] for the following three systems: (1) mutually saturated methyl methacrylate monomer–water interface; (2) system 1 with the addition of nonionic surfactant to the aqueous phase. For this purpose Igepal Co-990 in concentration of 0.8% (or Pluronic F-108 in concentration of 0.366%) by weight based on water was used in order to simulate the prevailing conditions during the second-stage polymerization. (3) System 2, where a polymer PS (or PMMA) was added to the monomer phase in increased concentrations while keeping the surfactant concentration in aqueous phase unchanged.

RESULTS AND DISCUSSION

Interfacial Tension of Polymer Phase–Water Interface

The interfacial tensions for PS190 in MMA—water and PMMA-KS in MMA—water are plotted in Figure 2. The results show that the interfacial tension initially decreases with increasing polymer concentration, followed by a plateau region in which the

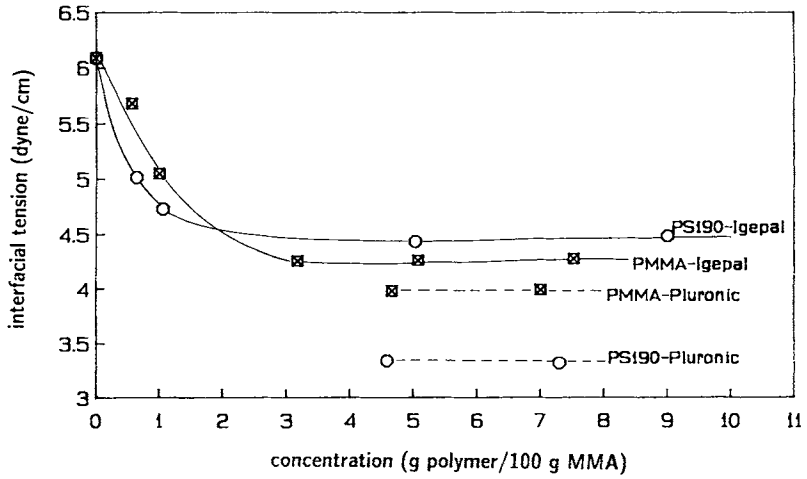

Figure 2 Interfacial tensions for PS190 in MMA–water and PMMA-KS in MMA–water systems at 25°C using Igepal Co-990 and Pluronic F-108 as surfactants, as a function of polymer concentration in MMA monomer.

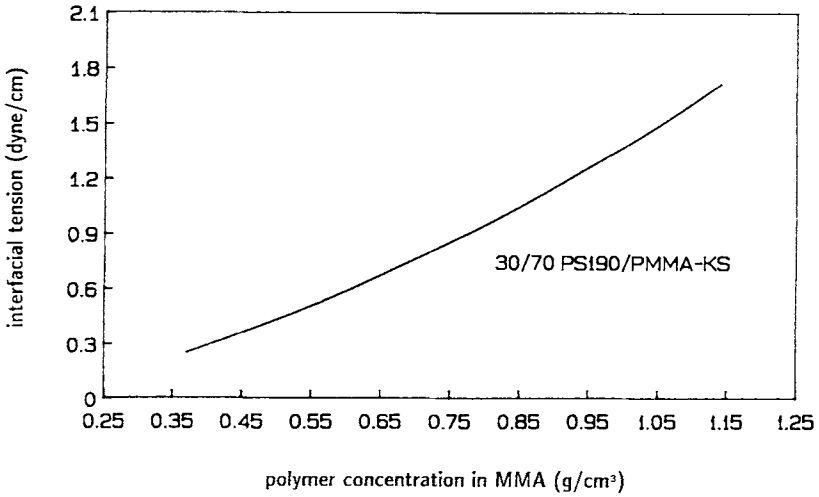

Figure 3 The calculated interfacial tensions of 30/70 weight ratio of polymer 1–polymer 2 system of PS190/PMMA-KS as a function of polymer concentration in MMA monomer.

interfacial tension stays constant with increasing the polymer concentration. This is because the polar components of polymer chains (e.g., polymer chains with SO_4 end groups) are more surface active than the nonionic surfactants and contribute to the initial decrease in interfacial tension. It seems that the sulfate-containing polymer chains displace the surfactant at the interface thus increasing the polarity of the interface between polymer (in monomer) and water, until the polarity reaches a certain equilibrium point depending on the amount and nature of the polar components of the polymer. The results in Figure 2 show that when surfactant Igepal Co-990 was used in the interfacial tension measurements, the PMMA-KS polymer exhibited a lower equilibrium interfacial tension (4.26 dyn/cm) than PS190 polymer (4.46 dyn/cm). On the other hand, when Pluronic F-108 was used during the interfacial tension measurement, the PS190 polymer showed a lower equilibrium interfacial tension (3.34 dyn/cm) compared to PMMA-KS polymer (3.98 dyn/cm). The impact of these differences in the interfacial tensions in the presence of the two types of surfactants on the particle morphology was investigated theoretically and experimentally; the results are given in the following sections.

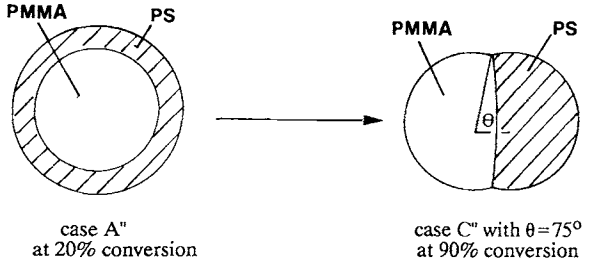

Figure 4 Schematic representation of the thermodynamically predicted morphology for PS190/PMMA/Pluronic system; as the conversion increases from 20 to 90%, the morphology changes from A″ to C″ with $\theta = 75°$.

Prediction of Particle Morphology and Experimental Verification

Based on the methodology reported in our previous work,[1,2] the composite particle configurations of the PS190/PMMA/Pluronic and PS190/PMMA/Igepal systems at 30/70 polymer weight ratio were predicted using the equations listed in Table I. The calculation of the free energy change for each case was done by a FORTRAN77 computer program. The required interfacial tensions between polymer phases 1, 2, and water containing the appropriate surfactant were determined from Figure 2. The in-

Table IV Morphological Configurations of PS190/PMMA/Pluronic System at 30/70 Polymer Weight Ratio[a]

Conversion %	γ_{12} (dyn/cm)	Case Predicted
20	0.35	A″
40	0.59	A″
45	0.66	C″ θ = 155°
50	0.73	C″ θ = 124°
90	1.48	C″ θ = 75°

[a] γ_{1w} = 3.34 dyn/cm, γ_{2w} = 3.98 dyn/cm.

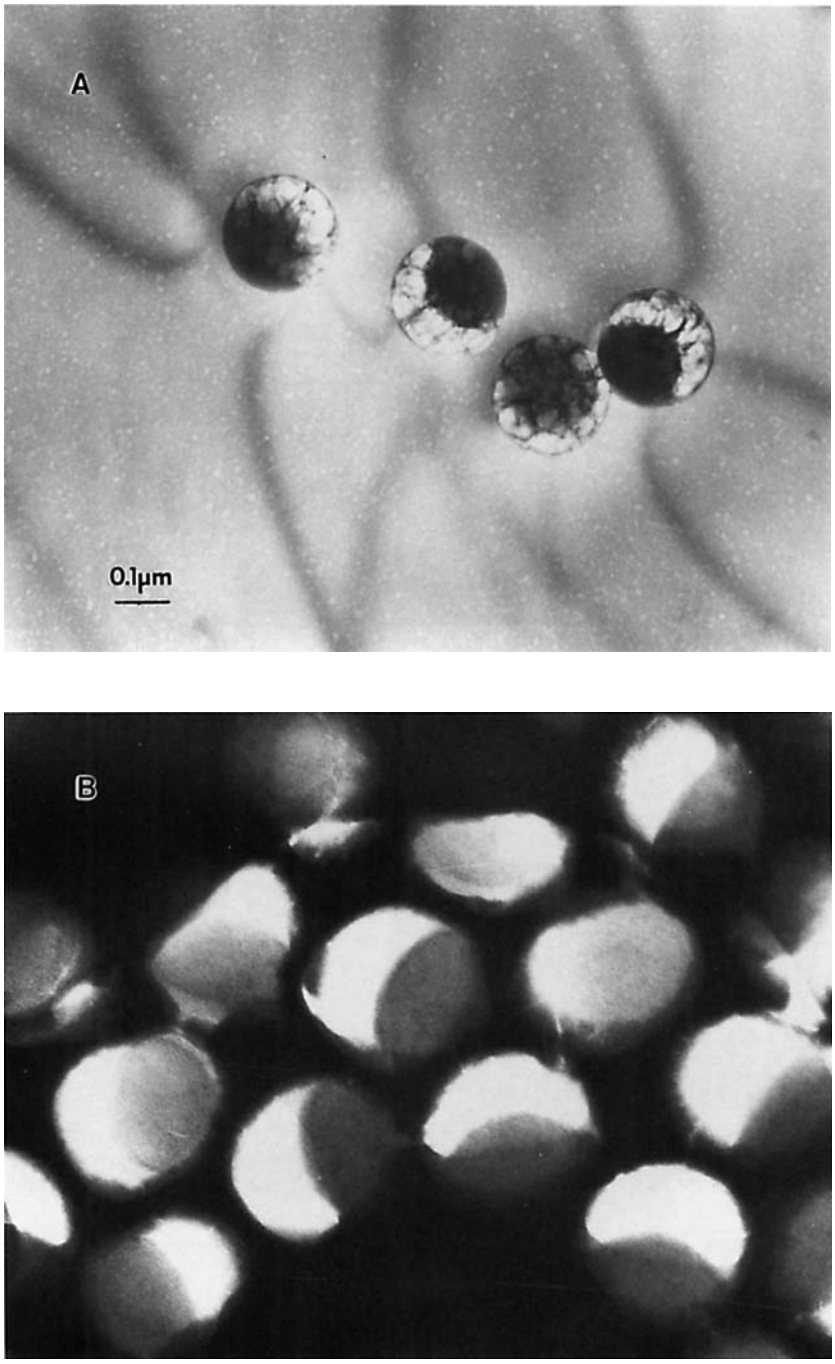

Figure 5 TEM of PS190/PMMA/Pluronic composite particles, after 30 min of polymerization (<20% conversion). (a) Particles embedded in ice; darker region, PS, was covered by the PMMA, lighter region. (b) Dry composite particles; dark regions are polystyrene stained with RuO_4 and lighter regions are PMMA domains outlined using phosphotungstic acid stain.

terfacial tensions at the plateaus were used. The interfacial tensions between polymer phase 1 and polymer phase 2, both in the second-stage monomer of MMA, were estimated from Figure 3 at the appropriate polymer concentrations. Figure 3 shows the calculated interfacial tensions between the two

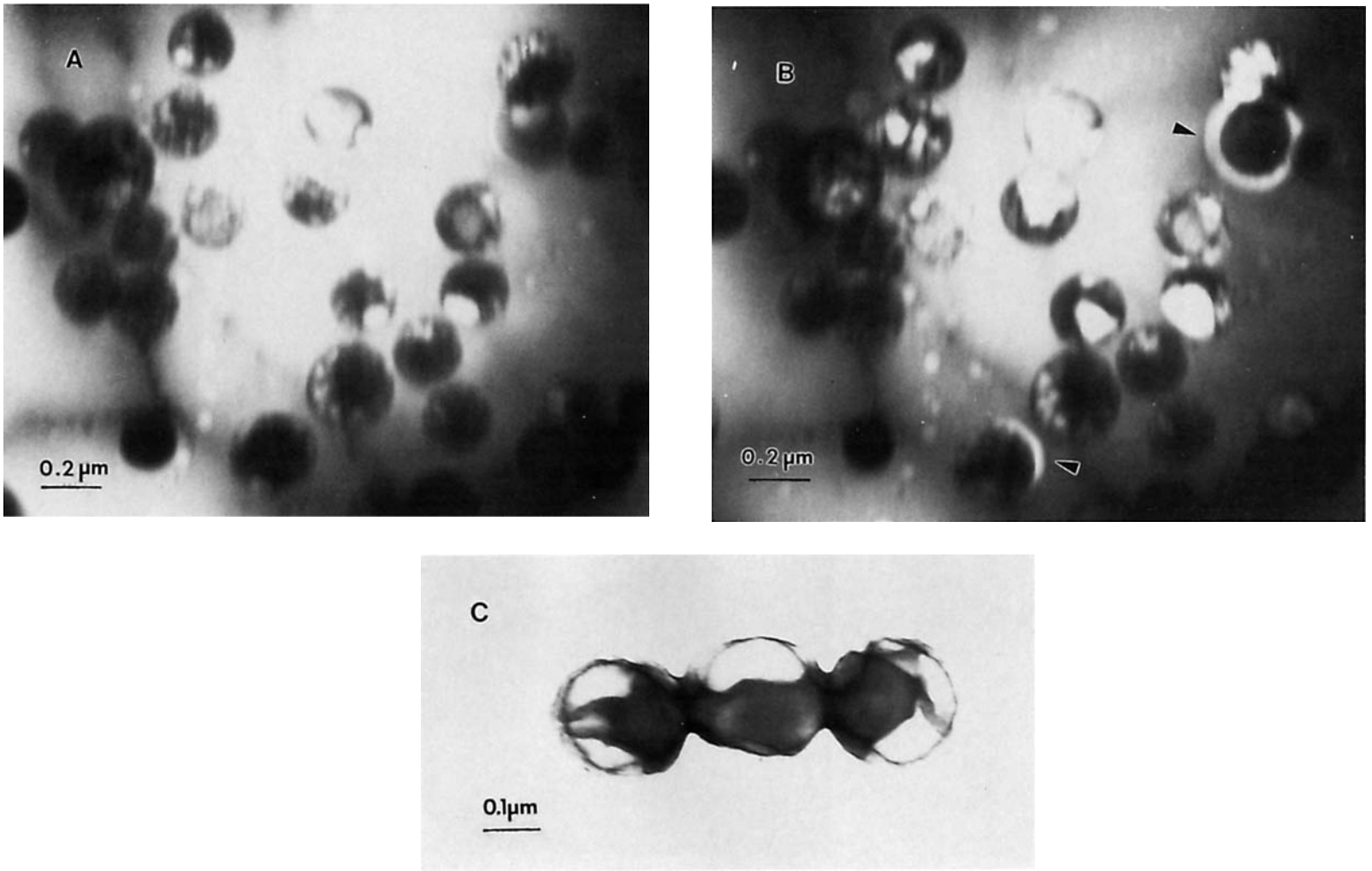

Figure 6 TEM of PS190/PMMA/Pluronic composite particles, after 1 h of polymerization (43% conversion). (a) Particles embedded in ice; lighter region, PMMA, was covered by PS, darker region. (b) Increased exposure time cause formation of cavities around PS phase and "swelling" of PMMA phase into the cavity. (c) Dry composite particles; dark regions are polystyrene stained with RuO_4 and lighter regions are PMMA domains outlined using phosphotungstic acid stain.

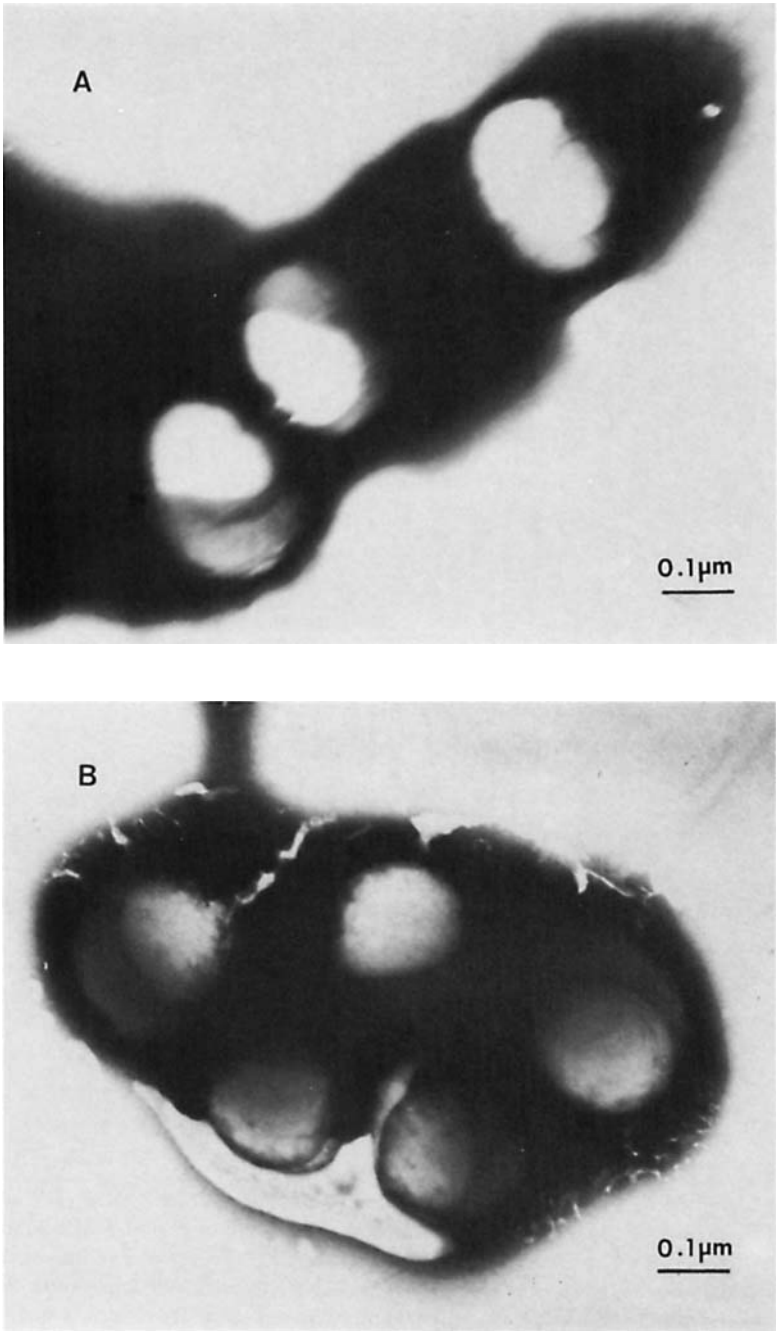

Figure 7 TEM of PS190/PMMA/Pluronic dry composite particles (a) after 2 h of polymerization (71% conversion), (b) after 2 h and 30 min of polymerization (90% conversion). Dark regions are polystyrene stained with RuO_4 and lighter regions are PMMA domains outlined using phosphotungstic acid stain.

polymer phases as a function of polymer concentration in MMA monomer for PS190/PMMA-KS system at 30/70 weight ratio of seed–monomer. These calculated polymer phase 1–polymer phase 2 interfacial tensions were based on the work of Broseta et al.,[15] according to the approach outlined previously.[2]

Figure 4 shows a schematic representation of the thermodynamically predicted morphology for PS190/PMMA/Pluronic system at 20 and 90%

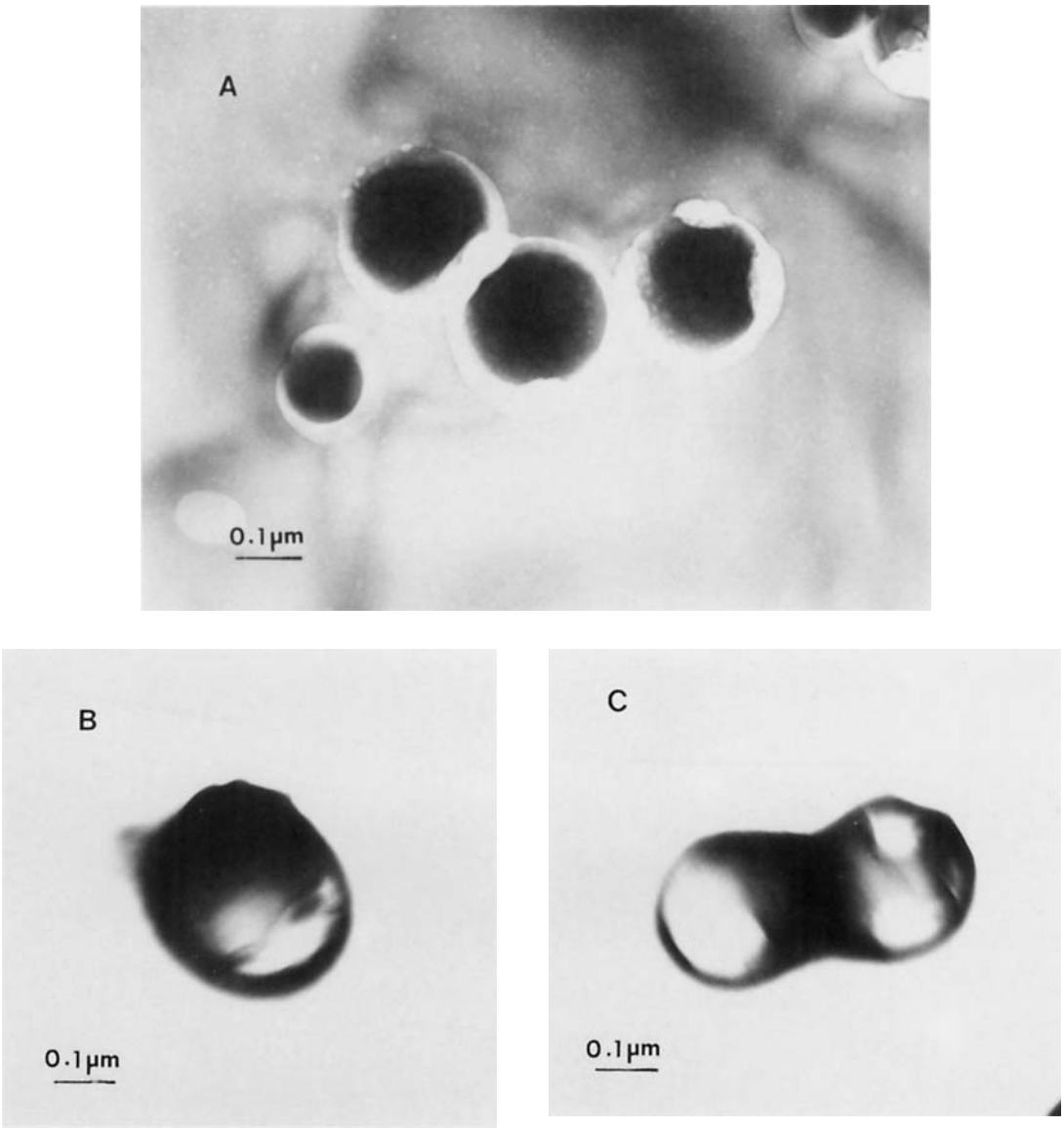

Figure 8 TEM of PS190/PMMA/Pluronic composite particles, after 3 h of polymerization (98% conversion). (a) Particles embedded in ice; lighter region, PMMA, was covered by PS, darker region. The formation of cavities around PS phase and swelling of the PMMA phase into the cavity were observed. (b) (c) Dry composite particles; dark regions are polystyrene stained with RuO_4 and lighter regions are PMMA domains outlined using phosphotungstic acid stain.

conversion of the second-stage MMA monomer. Table IV lists the interfacial tension γ_{12} and the thermodynamically predicted morphologies for the PS190/PMMA/Pluronic system at the 30/70 weight ratio as a function of the second-stage monomer conversion. As the second-stage monomer conversion increases from 20 to 90%, the polymer phase 1–polymer phase 2 interfacial tension also increases, and therefore the predicted morphology configuration changes from A″ (i.e., inverted PMMA core and PS shell) to case C″ with $\theta = 75°$ (i.e., part of the PMMA core particle surface is covered by PS domains).

The particle morphology of PS190/PMMA/Pluronic system as a function of percent conversion of the second-stage MMA monomer was examined by transmission electron microscopy using preferential staining of PS domains by RuO_4. Figure 5

shows the transmission electron micrographs of the composite particles after 30 min of polymerization where the conversion of MMA was less than 20%. Figure 5(a) shows the observed particle morphology by using the "embedded in ice" technique. One can see that the PMMA (lighter region) is partially covering the PS seed particle surface (darker region). The corresponding "dry" latex particle morphology in Figure 5(b) also shows that the PMMA polymer (lighter region) appears on the particle surface and partially covers the PS seed particle (darker region). The morphology shown in Figure 5 is indeed different from the expected inverted core–shell morphology (case A″) based on the thermodynamic analysis (Table IV). This difference is a manifestation of the role of the kinetics and mechanism of seeded emulsion polymerization. Because a water-soluble initiator, $K_2S_2O_8$, was used in the preparation of the composite latex particles, at low conversions (less than 20%) some of the polymerization of the MMA monomer tend to take place in the aqueous phase or at the particle surface. Due to these mechanistic and kinetic effects and perhaps the existence of some grafting reactions with the nonionic surfactant molecules,[16,17] it seems that at lower conversions the morphology of the composite latex particles with a predicted case A″ or even C″ structure is less favorable, as observed in Figure 5.

As the polymerization time and the conversion, increases further (above 40%), based on the thermodynamic model prediction (Table IV), the PMMA phase is expected to be partially engulfed by the PS phase due to the increase in γ_{12}, however, the area of the PMMA phase to be covered by PS phase is expected to be dependent on the phase mobility related to internal viscosity. Figure 6 shows the particle morphology after 1 h of polymerization (43% conversion). From the dry latex particle morphology shown in Figure 6(c), one can see the PMMA phase (lighter region) is now almost covered by PS phase (darker region). The same morphology can be also observed in Figures 6(a) and 6(b), showing the morphology of particles embedded in ice. As the exposure time to electron radiation increases [Fig. 6(b)], the PS domains (darker region) tend to form a crosslinked polymer network when directly irradiated. Therefore, the formation of cavities by etching of the ice around the PS phase (shell) can be observed in Figure 6(b) (see arrows). In addition, the PMMA underwent chain scission under direct irradiation, thus causing the "swelling" of PMMA phase into the cavity that is formed by the etching of ice. This effect can be also observed in Figure 6(b) where, compared with Figure 6(a), the PMMA phase (lighter region) is enlarged and it seems that more of the PMMA is covered by PS.

Figures 7(a) and 7(b) show the dry latex particle morphology after 2 h (71% conversion) and 2 h and 30 min (90% conversion) of polymerization, respectively. In these micrographs it is evident that the particle morphology now coincides qualitatively with the predicted case C″ morphology, where the PMMA phase (lighter region) is partially covered by PS phase (darker region).

The final particle morphology at 98% conversion after 3 h of polymerization for PS190/PMMA/Pluronic system at 30/70 polymer–monomer weight ratio is shown in Figure 8. From the micrograph of particles embedded in ice shown in Figure 8(a), one can see the continuous cavities surrounding the PS shell and only a few small lumps on the surface corresponding to PMMA domains. This configuration correlates well with the dry latex particle morphology shown in Figures 8(b) and 8(c) where the PMMA second-stage polymer (lighter region) is partially engulfed by the seed polystyrene (darker region). This degree of phase separation (θ angle around 140°) in the final composite particle is closer to the thermodynamically predicted morphology for lower conversions (see Table IV). This discrepancy could be due to the existence of some grafting between the polymer and the Pluronic surfactant, and a reduced-phase mobility or polymer chain mobility as a result of increased internal particle viscosity at high conversion. However, the observed type of encapsulation, PMMA engulfed by PS, shows a good qualitative agreement with the model prediction of case C″ type morphology.

Table V shows the predicted and observed morphologies for the PS190/PMMA/Igepal system using Igepal surfactant. The predicted morphology was case C (see Fig. 1) with θ angle 89°. The final morphology of the composite particles for this system can be observed in the transmission electron micrographs given in Figure 9. The micrograph in Figure 9(a) shows that case C morphology is prevailing where the second-stage PMMA (lighter region) is

Table V Morphological Configuration of PS190/PMMA/Igepal System at 30/70 Polymer Weight Ratio[a]

Conversion %	γ_{12} (dyn/cm)	Case Predicted	Observed
90	1.48	C θ = 89°	C

[a] γ_{1w} = 4.46 dyn/cm, γ_{2w} = 4.66 dyn/cm.

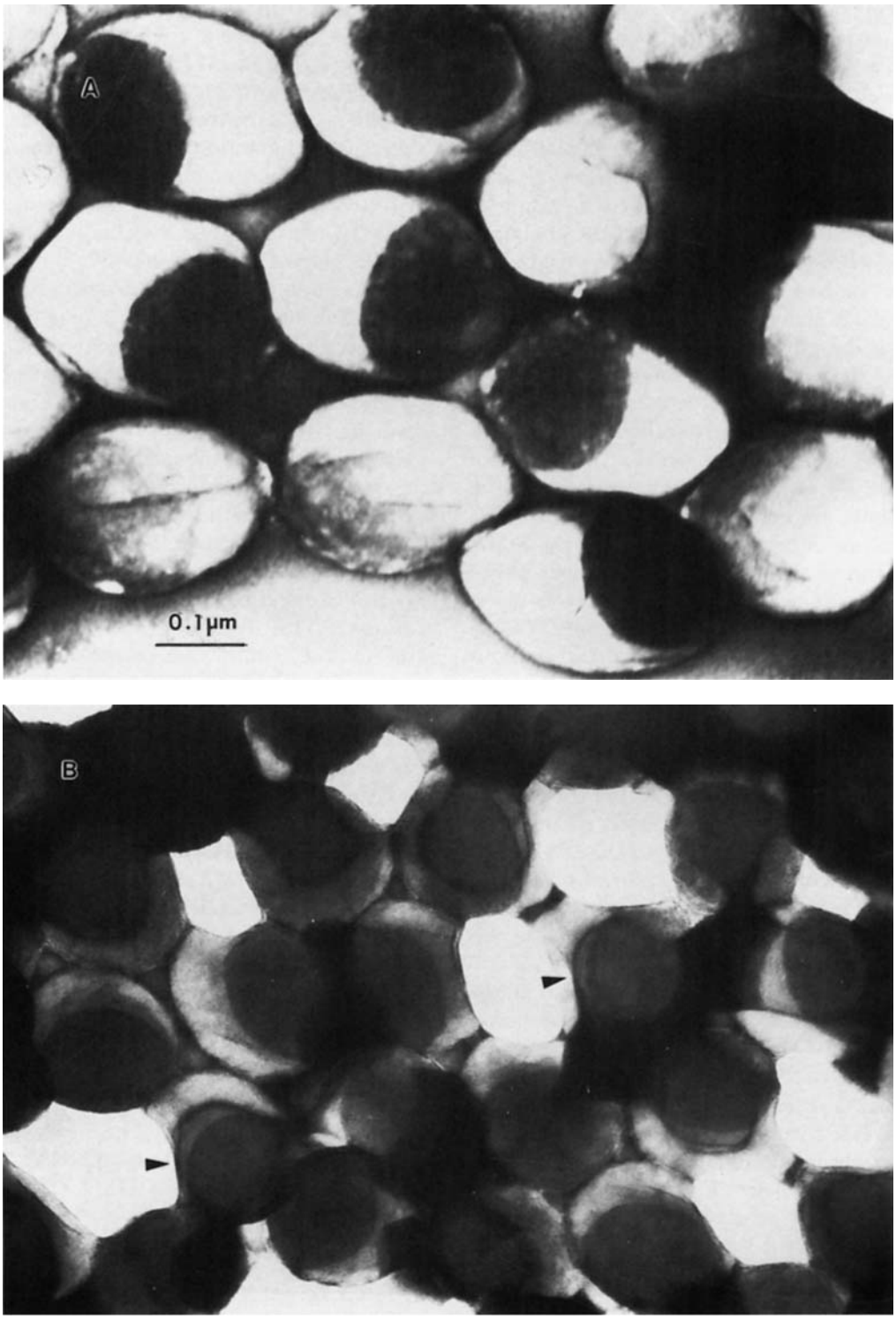

Figure 9 (a) TEM of PS190/PMMA/Igepal composite particles with 30/70 polymer weight ratio (98% conversion); darker region, PS, was covered by PMMA, lighter region. (b) As the PMMA was damaged by electron beam (▶), the spherical shape of PS190 was observed. Dark regions are polystyrene stained with RuO_4 and lighter regions are PMMA domains outlined using phosphotungstic acid stain.

partially covering the seed polystyrene (darker region). In Figure 9(b) where the composite particles are not fully embedded in PTA (particles marked by arrows), the PMMA domains suffered beam damage in the TEM and, therefore, the spherical shape of the PS core can be observed. The observed particle morphology corresponds quite well to the theoretical prediction of the model.

It is worth noting that the final composite latex morphologies of PS190/PMMA/Pluronic and PS190/PMMA/Igepal systems shown in Figures 8 and 9, respectively, agree well with the results of polymer phase–water interfacial tension measurements presented in Figure 2. This means that the interfacial tension of polymer phase against water (containing surfactant, if present) represents the important parameter in determining the type of encapsulation achieved under equilibrium conditions. The polymer with higher polymer phase–water interfacial tension have the tendency to be engulfed by the polymer with lower polymer phase–water interfacial tension.

CONCLUSIONS

Two systems of polystyrene–poly(methyl methacrylate) composite particles were prepared by seeded batch emulsion polymerization at 70°C using $K_2S_2O_8$ initiator and two different types of nonionic surfactants. In the first system, when Pluronic F-108 (polyethylene oxide–propylene oxide) was used, the final particle morphology showed the PMMA domains to be partially covered by polystyrene. However, in the second system, when Igepal Co-990 (nonylphenol polyethylene oxide) was used under the same polymerization condition of the first system, one observed a reversed type of encapsulation (i.e., PS is partially engulfed by PMMA). The interfacial tension of the polymer phase against water containing surfactant measured by drop-volume method was in good agreement with the observed particle morphologies. The phase with higher polymer phase–water (containing surfactant, if present) interfacial tension is engulfed by the phase with lower polymer phase–water interfacial tension.

The development of particle morphology during the course of polymerization was also observed by TEM. At higher conversion the particle morphology was in good agreement with predictions of the thermodynamic model. The kinetic factors and/or the grafting of the Pluronic surfactant by PMMA chains are considered to affect the particle morphology in the initial stage of polymerization, and thus cause deviation from the predicted morphology.

The assistance of Mrs. O. Shaffer with microscopy work, especially the morphology examination using "embedded in ice" approach, and guidance with photography are highly appreciated and acknowledged.

REFERENCES

1. Y. C. Chen, V. L. Dimonie, and M. S. El-Aasser, *Macromolecules,* **24,** 3779 (1991).
2. Y. C. Chen, V. L. Dimonie, and M. S. El-Aasser, *J. Appl. Polym. Sci.,* **42,** 1049 (1991).
3. V. L. Dimonie, M. S. El-Aasser, and J. W. Vanderhoff, *Polym. Mat. Sci. Engr.,* **58,** 821 (1988).
4. M. Okubo, Y. Katsuta, and T. Matsumoto, *J. Polym. Sci. Polym. Lett. Ed.,* **18,** 481 (1980).
5. S. Lee and A. Rudin, *Markromol. Chem., Rapid Commun.,* **10,** 655 (1989).
6. S. Torza and S. Mason, *J. Colloid Interface Sci.,* **33,** 67 (1970).
7. D. Sundberg, A. P. Casassa, J. Pantazopoulos, and M. R. Muscato, *J. Appl. Polym. Sci.,* **41,** 1425 (1990).
8. J. Guillot, *Acta Polym.,* **32,** 593 (1981).
9. J. Delgudo, M. S. El-Aasser, C. A. Silebi, J. W. Vanderhoff, and J. Guillot, *J. Polym. Sci. Polym. Phys.,* **26,** 1495 (1988).
10. D. I. Lee and T. Ishikawa, *J. Polym. Sci. Polym. Chem. Ed.,* **21,** 147 (1983).
11. O. Shaffer, M. S. El-Aasser, and J. W. Vanderhoff, 41st Ann. Mtg. Electron Microscopy Soc. Am., 30 (1983).
12. Y. Talmon, H. T. Davis, L. E. Scriven, and E. L. Thomas, *Rev. Sci. Instr.,* **50,** 698 (1979).
13. Y. Talmon, *Ultramicroscopy,* **14,** 305 (1984).
14. J. L. Lando and H. T. Oakley, *J. Colloid Interface Sci.,* **25,** 526 (1967).
15. D. Broseta and L. Leibler, *J. Chem. Phys.,* **87,** 7248 (1987).
16. I. Garat, V. Dimonie, D. Donescu, C. Hagiopol, M. Mnuteanu, K. Gosa, and T. Deleanu, *J. Polym. Sci. Polym. Symp.,* **64,** 125 (1978).
17. D. Donescu, I. Deaconescu, and K. Gosa, *Rev. Roam. Chim.,* **29,** 483 (1984).

Received March 15, 1991
Accepted August 1, 1991